ELSEVIER

Int. J. Therm. Sci. 41 (2002) 673–681

International Journal of Thermal Sciences

www.elsevier.com/locate/ijts

Heat transfer characteristics at an axial tube in a circulating fluidized bed riser ☆

Ajit Kumar Kolar [a,*], R. Sundaresan [b]

[a] *Heat Transfer and Thermal Power Laboratory Department of Mechanical Engineering, Indian Institute of Technology Madras, Chennai 600 036, India*
[b] *Department of Mechanical Engineering, Vellore Institute of Technology, Vellore 632 014, India*

Received 26 October 2001; accepted 8 February 2002

Abstract

Experimental surface-average heat transfer coefficients of a vertical tube located at various positions along the axis of a Circulating Fluidized Bed riser (CFB) are presented. Experiments were carried out on the tube in a 100 mm × 100 mm cross-section and 5.5 m tall CFB cold unit using silica sand of mean particle size 363 μm as the bed material. The copper tube was 9.6 mm OD and 0.6 m high placed in the core of the riser with hot water flowing though it. The tube was located axially at distances of 0.97 m, 1.62 m, 3.0 m and 4.0 m from the distributor plate. The fluidizing air velocity and solid circulation flux were varied in the range of 4.5–7.3 $m{\cdot}s^{-1}$ and 21–72 $kg{\cdot}m^{-2}{\cdot}s^{-1}$ respectively. The measured average heat transfer coefficient varied in the range of 58–101 $W{\cdot}m^{-2}{\cdot}K^{-1}$ and showed a decreasing trend from the riser bottom to the riser exit. At a given location, increasing the fluidizing velocity resulted in reduced heat transfer coefficient while increasing the solid circulation flux enhanced it. At a given average suspension density, the local dynamics of gas and solids adjacent to the tube surface affected the heat transfer. Gas convective contribution was found to be substantial at high gas velocities especially at higher tube locations. Using the experimental data for the axial tube, two empirical heat transfer correlations were developed in terms of the important design and operating parameters including a non-dimensional height parameter. Comparisons were made with literature available under similar but not identical operating parameters.

Keywords: Circulating fluidized bed riser; Heat transfer coefficient; Vertical tube; Axial location; Heat transfer ratio; Correlation

1. Introduction

In the last few years, several power plants based on Circulating Fluidized Bed (CFB) boiler technology have entered commercial service and are operating successfully with excellent pollution control capability, fuel flexibility and load control, the largest of these being the 250 MW_e plant operating since 1996 at Gardanne in France. The heat extraction in a commercial CFB boiler is generally accomplished in the water walls of the furnace. As the capacity of the boiler increases, the increased heat transfer surface area makes it imperative to increase the height of the furnace in addition to increasing of the cross-sectional area of the furnace. However it is desirable to restrict the height of the furnace to about forty meters due to commercial constraints. In such a case, additional heat transfer surface area is to be provided to complement the furnace wall area in order to accomplish the required heat absorption for the production of superheated steam. This is sought to be accomplished in practice by providing: (i) an External Heat Exchanger (EHE) at the bottom of the cyclone dipleg before recirculation of solids and/or (ii) in-furnace heat exchangers suspended in the core space of upper dilute zone of the riser in the form of wing walls, omega panels, and a division or a curtain wall [1]. The EHE is basically a bubbling fluidized bed heat exchanger, comprising of tube bundles immersed in the bed of particles caught by the cyclone, and operating as an economizer or a superheater. A knowledge of the heat transfer behaviour in different extraction methods is essential for a proper design and operation of a CFB boiler.

☆ This article is a follow-up to a communication presented by the authors at the ExHFT-5 (5th World Conference on Experimental Heat Transfer, Fluid Mechanics and Thermodynamics), held in Thessaloniki in September 24–28, 2001.

* Correspondence and reprints.
E-mail addresses: kolar@iitm.ac.in (A.K. Kolar), sunds60@hotmail.com (R. Sundaresan).

1290-0729/02/$ – see front matter
PII: S1290-0729(02)01362-5

Nomenclature

A_s	surface area of single vertical tube	m^2	
C_{pw}	specific heat of water	$J{\cdot}kg^{-1}{\cdot}K^{-1}$	
d_t	diameter of heat transfer tube	m	
d_p	particle mean diameter	m	
G_s	external solid circulation flux	$kg{\cdot}m^{-2}{\cdot}s^{-1}$	
H_b	height of bed	m	
H_d	height from the distributor plate to midpoint of the heat transfer tube	m	
H_t	height of the heat transfer tube	m	
h	total (gas convective plus particle convective) surface-average convective heat transfer coefficient	$W{\cdot}m^{-2}{\cdot}K^{-1}$	
h_{gc}	gas convective heat transfer coefficient	$W{\cdot}m^{-2}{\cdot}K^{-1}$	
k_g	thermal conductivity of gas	$W{\cdot}m^{-1}{\cdot}K^{-1}$	
m_w	mass flow rate of water	$kg{\cdot}s^{-1}$	
Nu_p	particle Nusselt number $= hd_p{\cdot}kg^{-1}$		
Q	rate of heat transfer	W	
Re_p	particle Reynolds number	$Ud_p\rho_g/\mu_g$	
T_b	average bed temperature	K	
T_s	average surface temperature of tube	K	
T_{wi}	inlet temperature of water	K	
T_{wo}	outlet temperature of water	K	
U	fluidizing gas velocity	ms^{-1}	

Greek symbols

ε	cross-sectional average voidage	
ρ_g	density of gas	$kg{\cdot}m^{-3}$
ρ_p	density of sand particles	$kg{\cdot}m^{-3}$
ρ_{sus}	cross-section average suspension density	$kg{\cdot}m^{-3}$
μ_g	viscosity of gas	$kg{\cdot}m^{-1}{\cdot}s^{-1}$
ΔH	distance between two-wall pressure taps	m
ΔP	pressure drop across height of heat transfer tube	Pa

2. Literature review

Extensive literature is available for heat transfer at the water wall of a CFB furnace [2,3], and in bubbling beds [4]. However, such heat transfer data is not applicable to the core heat transfer tubes in a CFB, since the flow pattern of the gas-solid mixture in the two cases is quite different. It is very well recognized that the CFB riser in general comprises of a very shallow "bottom dense bed" and a very deep "upper dilute zone". The latter zone exhibits both radial and axial voidage variation leading to the existence of a "core-annulus" structure of particle distribution. Therefore, a heat transfer tube placed in the core could be expected to exhibit heat transfer characteristics depending upon its radial and axial location, differing from that placed in the annulus formed on the wall. Radial variation of heat transfer coefficients in the core has been reported in literature. Some information is available on a single vertical tube [5–10] placed at the axis in the core region of a CFB, and pertinent data is presented in Table 1. It is observed that only Kiang et al. [5] and Minicic et al. [10] have reported data on the axial variation of the heat transfer coefficient.

Experiments of Kiang et al. [5] were focused on short vertical heaters (57 mm long), using small FCC particles (53 μm), and relatively low fluidizing velocities (upto 4.9 $m{\cdot}s^{-1}$). The measured heat transfer coefficients varied from 45 to 230 $W{\cdot}m^{-2}{\cdot}K^{-1}$ in the H_d/H_b range of 0.15–0.86. The external solid circulation flux was not measured but was indirectly reported as a certain percentage of the recycle valve opening. The overall bed density was not clearly indicated but appears to be in the range of 20–40 $kg{\cdot}m^{-3}$ for fluidizing velocities lower than 2.5 $m{\cdot}s^{-1}$. They claimed "relatively uniform heat transfer coefficient in the bed" although the data indicated substantial variation with axial location. Mincic et al. [10] did not specify the size of the heat transfer tube but used small particles (150 μm) and low fluidizing velocities (upto 4.4 $m{\cdot}s^{-1}$) and reported an overall bed suspension density of 80 $kg{\cdot}m^{-3}$ and heat transfer coefficients in the range of 70–270 $W{\cdot}m^{-2}{\cdot}K^{-1}$ when the H_d/H_b varied from 0.16–0.72. The external solid circulation rate was not measured. They demonstrated that there is a substantial variation of the heat transfer coefficient along the axis, including for the data of Kiang et al. [5]. The length of the heat transfer tubes in these two investigations appear to be small enough for the heat transfer coefficients to be considered as local values.

In normal CFB boiler practice, the particle size is in the range of 150–360 μm, the fluidizing velocity varies between 4–7 $m{\cdot}s^{-1}$, and the suspension density varies between 10–20 $kg{\cdot}m^{-3}$ in the upper dilute region where the water wall exists. The height of the core heat exchangers, if provided in some designs, is about 10% of the bed height. However, the design and operating conditions of the CFB in the experiments of Kiang et al. [5] and Mincic et al. [10] are considerably different from what is applicable to a CFB boiler. Additionally, they did not measure the solids recycle rate and also reported only the overall bed suspension density along the entire bed height, which is different from the suspension density existing in the region of the tube height.

In this context, an attempt is made in the present investigation to study the variation of surface-average heat transfer coefficient over a vertical tube located at various axial positions in the CFB riser. Specifically, the heat transfer tube is 600 mm long occupying about 11% of the bed height and

Table 1
Heat transfer at axial tubes—literature data

Ref.	CFB riser (mm)	Bed height H_b (m)	Heat transfer tubes			H_d/H_b	U ($m\cdot s^{-1}$)	G_s ($kg\cdot m^{-2}\cdot s^{-1}$)	h ($W\cdot m^{-2}\cdot K^{-1}$)
			d_t (mm)	H_t (m)	H_d (m)				
Kiang et al. [5]	Cold 100 dia	3.66	19	0.057	0.56	0.153	0.5–4.9	–	45−230
					1.32	0.360			
					2.39	0.65			
					3.15	0.86			
Basu [6]	Hot 202 square	6.3	38	0.81	5.9	0.93	–	–	130−200
Zheng et al. [7]	Cold 112 dia	5.5	10	3.7	2.8	0.51	2.6–5.8	2−50	65−100
Bi et al. [8]	Cold 186 dia	8	10	0.04	3.0	0.38	2.5–6.0	20−150	60−420
				0.08					
				0.16					
				0.336					
Ahn and Han [9]	Cold 50 dia	2.5	4.75	0.9	1.8	0.72	2.5–6.0	20−100	40−80
Mincic et al. [10]	Cold 120 dia	5	–	–	0.8	0.16	2.5–4.4	–	62−321
					1.7	0.34			
					2.5	0.5			
					3.6	0.72			
Present work	Cold 100 Square	5.5	9.6	0.6	0.97	0.176	4.5–7.3	21−72	74−101
			9.6	0.6	1.62	0.295	4.5–7.3	21−72	69−98
			9.6	0.6	3.0	0.545	4.5–7.3	21−72	60−83
			9.6	0.6	4.0	0.727	4.5–7.3	21−72	58−75

the fluidizing velocity is varied in the range 4.5–7.3 $m\cdot s^{-1}$. The solids recycle rate was measured by using a special technique and the suspension densities were measured over the actual height of the tube

3. Experimental work

Fig. 1 shows the schematic diagram of the laboratory scale 100 mm × 100mm cold CFB facility. The major components of the facility were (i) CFB riser (ii) cyclone separator and (iii) a non-mechanical L-valve for recycle. The CFB riser was made of two sections: the bottom section, 700 mm high, which accommodated the air distributor and particle reinjection port, and the top section, which was 4.8 m in height. The recycle port was at a height of 450 mm from the distributor plate. The walls of the riser were made out of transparent Plexiglas material to facilitate flow visualization. The CFB riser outlet was connected to a high efficiency cyclone separator through a smooth bend to avoid an abrupt exit of the particles. The bottom of the cyclone separator was connected to the solid circulation rate measuring section through the cyclone dipleg. The solid circulation rate was measured by closing the butterfly valve placed in this section and measuring the volume of solids collected in the graduated column above it over a certain time interval.

The heat transfer tube was of 9.6 mm OD copper tubing, 0.6 m high placed at four axial positions of the CFB riser: 0.97 m, 1.62 m, 3.0 m and 4.0 m from the distributor plate, giving a range of non-dimensional height ratio H_d/H_b from 0.1 to 0.7. A constant temperature bath provided with a temperature controller was used to supply hot water (70 to 80 °C) to the heat transfer tube and a rotameter was used to measure the flow rate. Calibrated Copper-Constantan thermocouples of 0.2 mm size were used to measure the temperature of the tube surface at two locations, and of water at inlet and outlet. The bed temperatures were measured at the top, middle and bottom of the tube height in the vicinity of the tube surface. All the thermocouples were connected to a digital millivoltmeter through a selector switch. The entire riser column was provided with twenty-four wall static pressure tappings connected to a water tube manometer for the measurement of axial pressure profile.

Experiments were conducted to determine the total (gas convective plus particle convective) surface-average heat transfer coefficient with the tube placed at the axis of the CFB riser. Hot water from the bath was made to flow through the tube after the establishment of particle circulation in the riser by controlling the independent variables, namely the fluidizing velocity and the solid circulation flux. After steady state was reached with respect to the water outlet condition, all the thermocouple outputs and the axial bed pressure profile were recorded. Experiments were conducted with 363 μm sand (density 2740 $kg\cdot m^{-3}$) for a range of fluidizng velocity (4.5–7.3 $m\cdot s^{-1}$), and solid circulation flux (21–72 $kg\cdot m^{-2}\cdot s^{-1}$). The total bed inventory was 20 kg for all the cases.

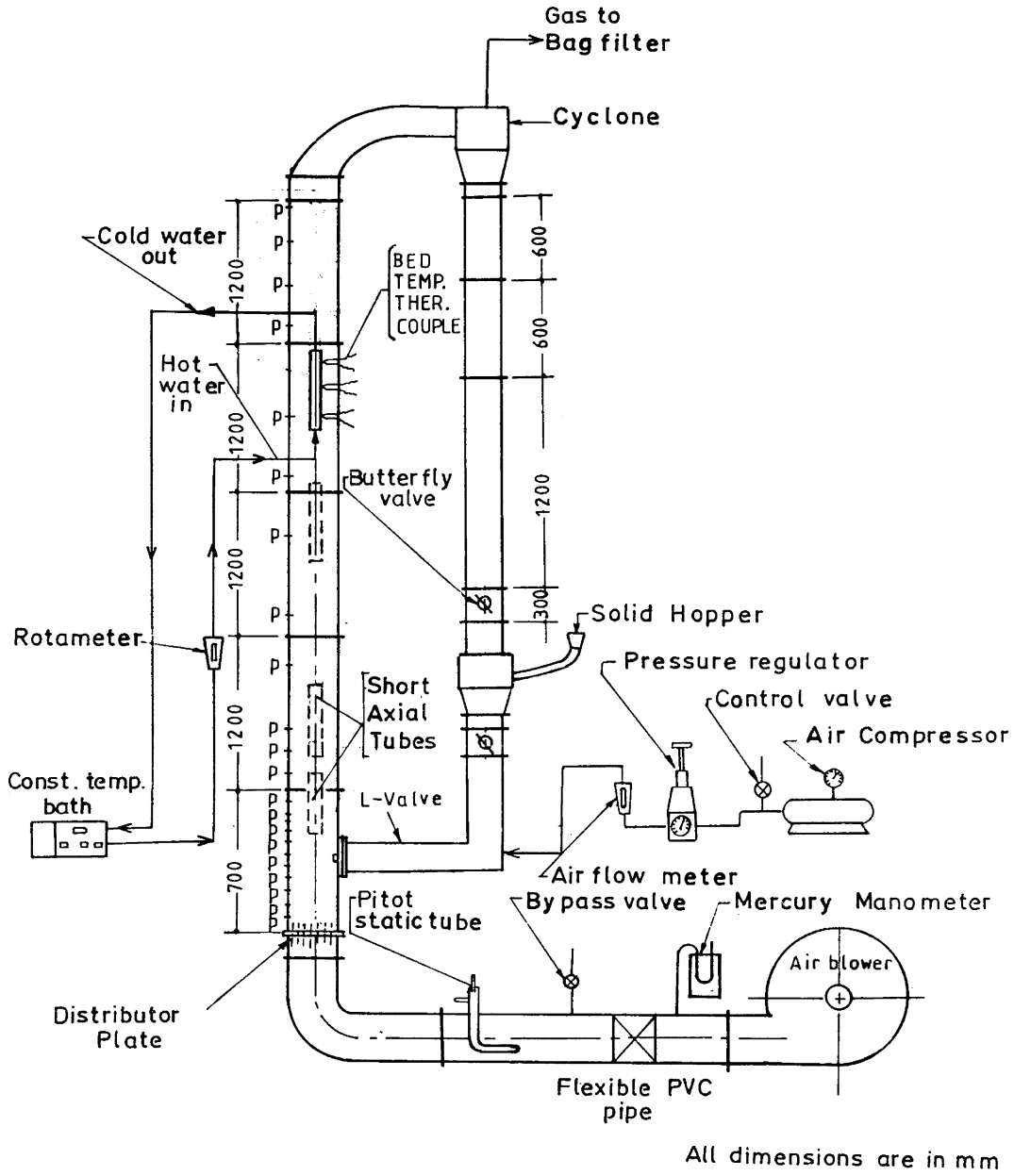

Fig. 1. Schematic of CFB experimental facility.

The cross-sectional average voidage was determined from the pressure drop ΔP on the riser wall measured across the height of the heat transfer tube as:

$$\varepsilon = 1 - \frac{\Delta P}{g\rho_p \Delta H} \tag{1}$$

where ΔH is the distance between two wall pressure tappings.

The cross-sectional average suspension density over the tube height, was determined from the relation:

$$\rho_{sus} = (1-\varepsilon)\rho_p \quad (\mathrm{kg\cdot m^{-3}}) \tag{2}$$

The total surface-average heat transfer coefficient between the tube surface and the bed was calculated as:

$$h = \frac{Q}{A_s(T_s - T_b)} \quad (\mathrm{W\cdot m^{-2}\cdot K^{-1}}) \tag{3}$$

where

$$Q = m_w c_{pw}(T_{wi} - T_{wo}) \quad (\mathrm{W}) \tag{4}$$

An error analysis showed that the heat transfer coefficient was measured within ±4.8% from Eq. (3).

4. Results and discussion

4.1. Suspension density profile

It is generally recognised that the cross-sectional average suspension density (calculated from the pressure drop measurement on the wall of the CFB riser) is the most significant characteristic affecting the heat transfer between the bed and the furnace water wall. Hence in literature the heat transfer coefficients are presented as a function of the average suspension density. However it should be noted that the suspension density is not an independent parameter but a derived one dependent upon the combination of the particle size, fluidizing velocity and the solids recycle rate for a given bed material, bed geometry and the bed hold up. Further, it may be relevant to point out that since the heat transfer is influenced by the gas and particle motion in the immediate vicinity of the heat transfer surface, the local suspension density is physically more meaningful than the cross-sectional average density. However, to facilitate discussion and comparison with the data reported in literature, the latter values obtained over the tube height are reported. The actual local suspension density at the axis is lower than these average values.

Fig. 2 shows the variation of suspension density derived from the measured ΔP along the CFB riser height. It is seen that within an initial portion of about one meter of the bed, the suspension density decreased drastically from about 320 to 50 kg·m^{-3} and thereafter gradually decreased to about 10 kg·m^{-3} very close to the riser exit, indicating a highly dispersed phase flow in the bed. The "bottom dense bed" with a voidage lower than about 0.725 as defined by Zijerveld et al. [11] is conspicuous by its absence, which is typical for small size CFB risers as in the present case, especially at high gas velocity and riser pressure drop less than 5.5 kPa. As per Zijerveld et al. [11] it would appear that the state of the circulating fluidized bed in the present work is the "intermediate dilute flow" which could be referred to as a fast fluidization regime without a bottom dense bed.

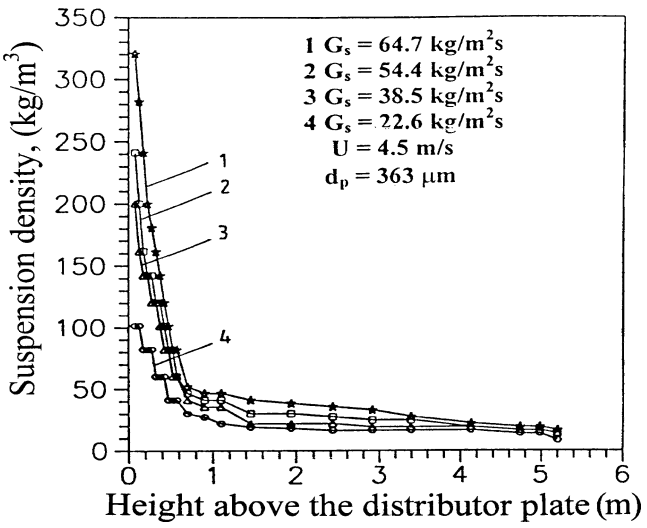

Fig. 2. Variation of suspension density along the CFB riser height.

4.2. Axial variation of heat transfer coefficient

Fig. 3 shows the variation of heat transfer coefficient with suspension density at four tube locations. It is observed that the heat transfer coefficient increases with suspension density as in the case of CFB wall heat transfer. This is due to the larger number of solid particles in a given volume at higher suspension densities and/or enhanced activity of the particles resulting in enhanced particle convection. It is also seen that at if the suspension density is held constant at different tube locations, the heat transfer coefficient varies, being the highest at the lower locations. This could be explained by the fact that the gas-solid particles motion is more vigorous in the lower regions of the riser. This indicates that the heat transfer coefficient is not uniquely dependent on the average suspension density, but the nature and extent of gas-solid particle motion is also a significant factor. This argument could be extended to hypothesize that at a given location and local suspension density, the heat transfer coefficient could vary depending on the surface characteristics like the surface roughness, as also indicated by Glicksman [2] for wall heat transfer.

Fig. 4 shows the effect of axial location on heat transfer coefficient along the CFB riser height for a solid circulation rate of 22 kg·m^{-2}·s^{-1} with U as a parameter. At any gas velocity, the heat transfer coefficient shows a maximum at the bottom and decreases towards the top due to the progressive decrease in suspension density. At any given location it is observed that higher gas velocities result in lower heat transfer coefficients. This may be attributed to particles being carried away from a given location due to the higher velocities resulting in lower suspension densities.

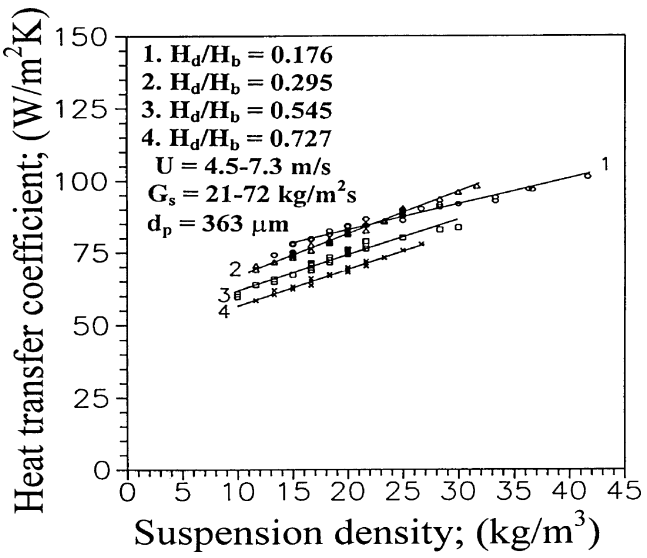

Fig. 3. Effect of suspension density on heat transfer coefficient at four tube locations.

4.2.1. Comparison

Axial heat transfer data under identical configuration and operating conditions is not available in the literature. However, Kiang et al. [5] and Mincic et al. [10] presented data on axial variation of (apparently) local heat transfer coefficient and these are compared with the present data of surface average heat transfer coefficient as shown in Fig. 5. It is observed that in all the cases there is a decline in the heat transfer coefficient from the bottom towards the top of the bed. The present data shows a fairly linear decline and also exhibits the lowest values while the other data exhibit non-linear inverse *S*-shaped profiles with Kiang et al. [5] data actually showing a point of inflection near the bottom of the bed. The maximum decline in heat transfer is indicated in the data of Mincic et al. [10], namely from 160 $W \cdot m^{-2} \cdot K^{-1}$ to 80 $W \cdot m^{-2} \cdot K^{-1}$. Kiang et al. [5] contended that the variation might be due to the large particle size distribution (that results in some inhomogenity in the bed) and end effects. The present study involved a narrow cut particle size distribution. Mincic et al. [10] attributed the variation of axial heat transfer coefficient to the *S*-shaped voidage distribution reported under their experimental conditions. For the present narrow-cut particle size of 363 μm the *S*-shaped voidage distribution was not observed. It is also observed from the figure that lower the particle size and shorter the heat transfer tube, the higher is the heat transfer coefficient.

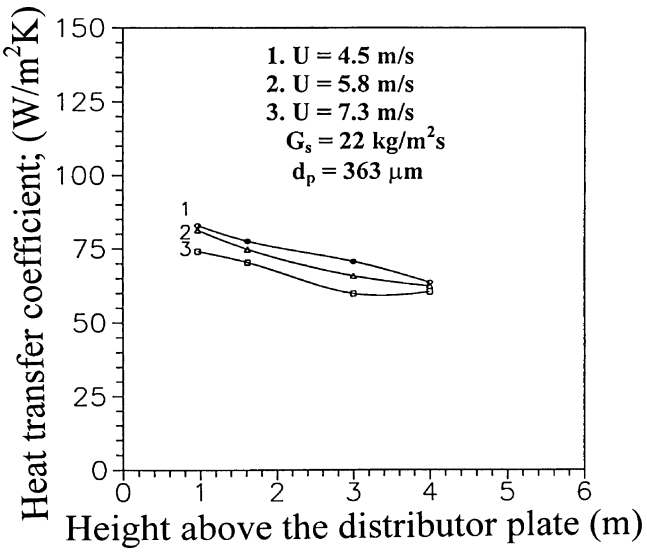

Fig. 4. Effect of axial location on heat transfer coefficient with *U* as a parameter.

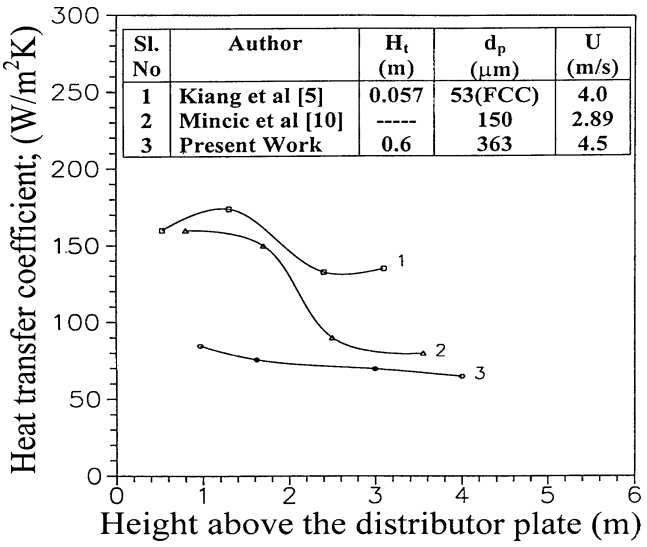

Fig. 5. Comparison of axial heat transfer data with published heat transfer results.

4.3. Effect of gas velocity

The influence of gas velocity on the heat transfer coefficient at various tube locations at a constant G_s value is shown in Fig. 6. It can be seen that the heat transfer coefficient decreases with increase of gas velocity at all the locations. This may be compared to the data reported [5,9] on core heat transfer coefficient which showed a similar trend. This behavior is a consequence of the reduction of the local suspension density at higher velocities. It is also noticed that at constant gas velocity, the heat transfer coefficient is higher at lower tube location. This may be attributed to the fact the local suspension density decreases along the height of the bed at any given velocity, resulting in a corresponding variation of heat transfer coefficient.

4.4. Effect of solid circulation flux

The effect of solid circulation flux on the heat transfer coefficient at various tube locations at a constant velocity is shown in Fig. 7. It is seen that the heat transfer coefficient at a given location increased with increase of solid circulation flux, which is a result of increased local suspension density.

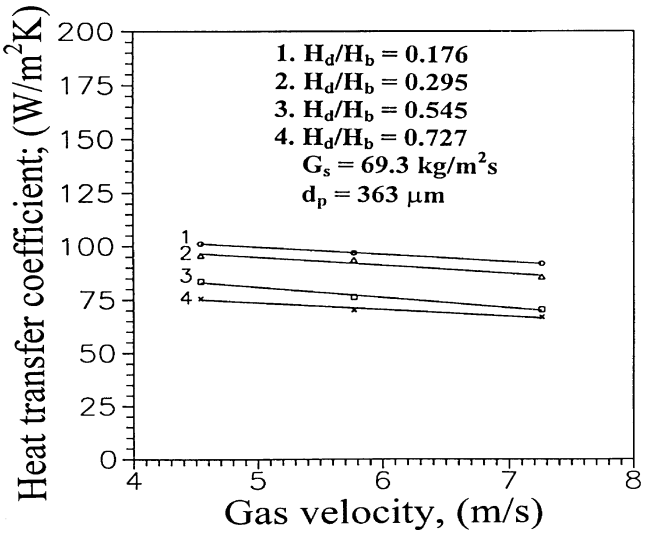

Fig. 6. Effect of gas velocity on heat transfer coefficient at four tube locations.

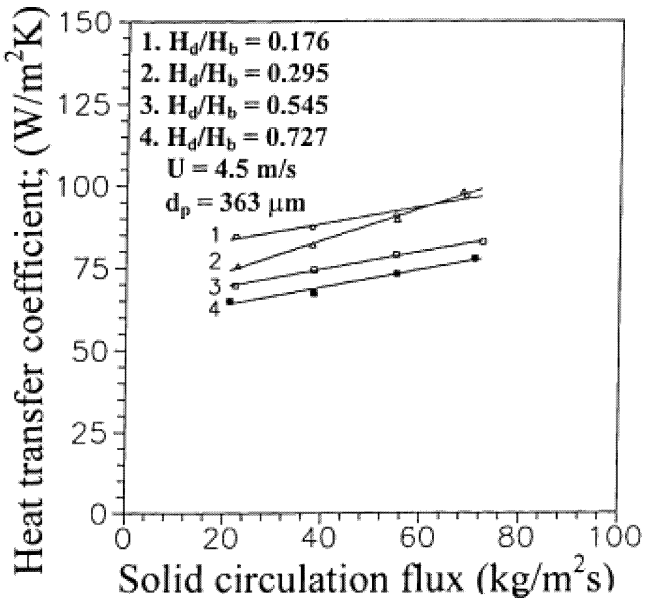

Fig. 7. Effect of solid circulation flux on heat transfer coefficient at four tube locations.

Increasing the solid circulation flux means more particles per unit surface area near the surface enhancing the heat transfer. Similar behavior is observed for other locations. Also at a given solid circulation flux, higher tube locations experience lower heat transfer coefficient because of lower local suspension densities.

4.5. Heat transfer ratio

It is generally recognized that the total heat transfer coefficient between a hot CFB and the core heat transfer surface is to a first approximation, the sum of the gas convective, particle convective and radiative components. Radiative component is negligible at low bed temperature and is absent in laboratory size cold beds. It will be interesting to evaluate gas convective component relative to the total convective heat transfer coefficient in the present experiments.

Experiments were conducted to measure the gas convective heat transfer coefficient for the tube located along the axis at various levels under "gas flow only" (without particles) condition in the gas velocity range of 4 to 8 $m \cdot s^{-1}$. These were in the range of 19 to 45 $W \cdot m^{-2} \cdot K^{-1}$. The experiments with particles in the bed under fluidizng conditions gave the total heat transfer coefficient 'h' as a function of particle size, gas velocity and solid circulation flux. From these, the heat transfer ratio h_{gc}/h was calculated and presented in Figs. 8 and 9 with G_s and U as parameters respectively at various tube locations.

The heat transfer ratio understandably depends on the interplay of the gas velocity, particle size and the solid circulation flux affecting the gas-solid motion near the heat transfer surface. From Fig. 8 it is observed that the gas convective component increased from about 20% at the

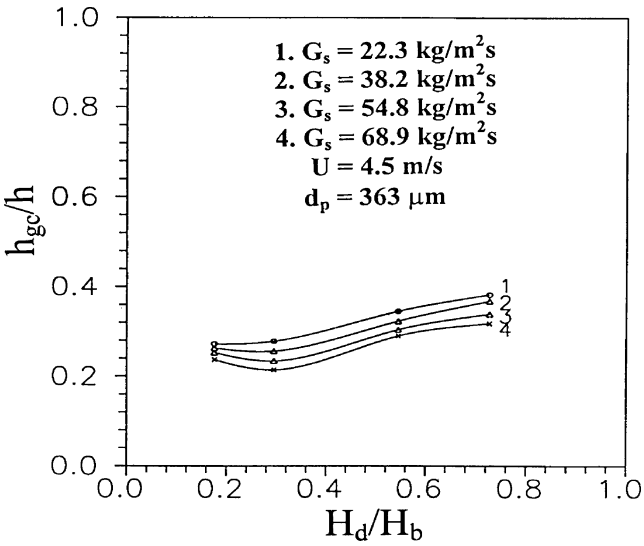

Fig. 8. Axial variation of heat transfer ratio with G_s as a parameter.

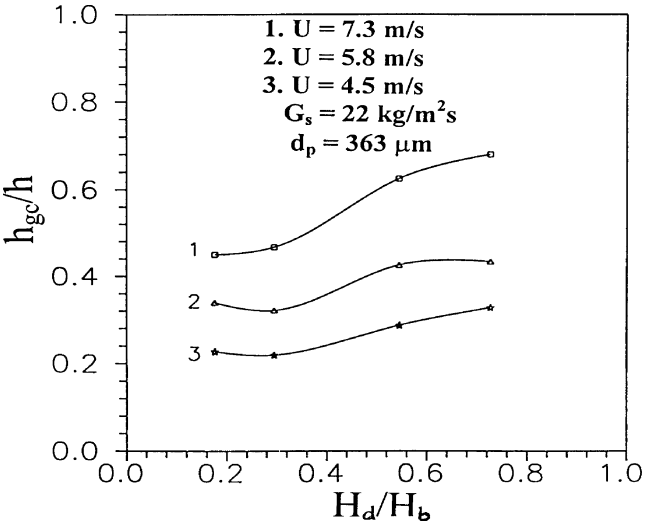

Fig. 9. Axial variation of heat transfer ratio with U as a parameter.

lower tube locations to a maximum of about 35% at the highest tube location for a given velocity and particle size. It also indicates that higher the solid circulation flux, the lower will be the gas convective component. Further in Fig. 9, it is observed that higher gas velocities increase the gas convective component from about 20% at the bottom of the CFB riser, for a given solid circulation rate, to a maximum of about 70% at the highest location. This behavior is obviously due to the extremely low suspension densities (of the order of 10 $kg \cdot m^{-3}$) close to the riser exit and the relatively higher suspension densities closer to the bottom of the bed. Clearly, the heat transfer coefficient is more sensitive to the change in gas velocity than that in the solid circulation flux, more prominently so at the highest location.

It is quite clear from the above that the heat transfer behavior is very strongly dependent on not only the local suspension densities but also on the degree of particle activity which influences the frequency and the time of

contact of particles and the tube surface. This gas-particle behavior is in turn dictated by (i) a combination of the three operating variables namely particle size, gas velocity and solid circulation flux and (ii) the axial location of the heat transfer tube.

5. Correlations

5.1. Particle Nusselt number

A dimensional analysis was made using Buckingham π theorem and ten possible non-dimensional numbers were derived. These were compared with dimensionless numbers used in published literature. Nusselt number and Reynolds number were identified as the most important and widely used numbers. Further based on the information from the literature as well as the authors' experience two more non-dimensional numbers were added. These are (a) a "non-dimensional density" number as given by cross-section average suspension density divided by the density of gas, (ρ_{sus}/ρ_g), and (b) a "non-dimensional height" number given by the ratio of the height from the distributor plate to midpoint of the heat transfer tube to the height of the bed (H_d/H_b). From this perspective, using the present data on the axial tube, the following correlation was developed with a correlation coefficient of 0.971:

$$Nu_p = a\left[\frac{U d_p \rho_g}{\mu_g}\right]^b \left[\frac{\rho_{sus}}{\rho_g}\right]^c \left[\frac{H_d}{H_b}\right]^d \tag{5}$$

where $a = 0.57$, $b = -0.063$, $c = 0.271$ and $d = -0.856$.

Fig. 10 shows the comparison of the present experimental results with the prediction of the above correlation showing a deviation of $\pm 5\%$. An analysis of the correlation reveals that the heat transfer coefficient varies as $U^{-0.063}$, $d_p^{-1.063}$, $(\rho_{sus})^{0.271}$ and $(H_d)^{-0.856}$ which are qualitatively meaningful and quantitatively appear reasonable. The strong effect of the tube location on the heat transfer coefficient is clearly indicated. It is also interesting to note that Ahn and Han [9] have indicated that the heat transfer coefficient varies as $(\rho_{sus})^{0.23}$ comparable with the present result. This correlation is valid in the following range of experimental conditions: $93 < Re_p < 153$, $9 < (\rho_{sus}/\rho_g) < 37$, $0.176 < (H_d/H_b) < 0.727$. The particle Nusselt number was in the range of 0.791 to 1.295.

5.2. Heat transfer ratio

A correlation was developed for the heat transfer ratio relating the suspension density, gas velocity, solids flux and tube location as follows:

$$\left[\frac{h_{gc}}{h}\right] = a\left[\frac{\rho_{sus}}{\rho_g}\right]^b \left[\frac{U}{U_t}\right]^c \left[\frac{G_s}{\rho_g U}\right]^d \left[\frac{H_d}{H_b}\right]^e$$

where $a = 0.266$, $b = -0.06$, $c = 1.333$, $d = -0.118$ and $e = 0.205$.

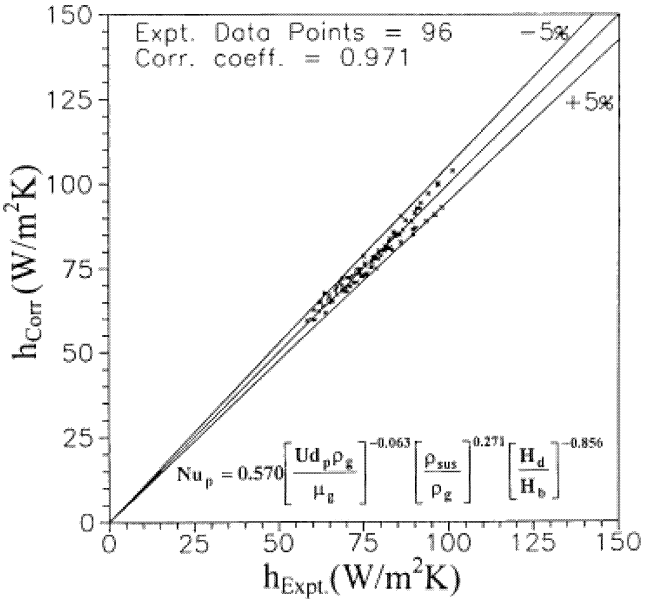

Fig. 10. Comparison of the experimental data with the proposed correlation for total surface-average heat transfer coefficient.

The correlation coefficient is 0.982 with a deviation of $\pm 10\%$. An analysis of the correlation reveals that the heat transfer coefficient varies as $U^{1.451}$, $(\rho_{sus})^{-0.060}$, $(H_d)^{0.205}$, and $G_s^{-0.118}$. This correlation is valid in the following range of experimental conditions:

$10 < (\rho_{sus}/\rho_g) < 37$, $1.698 < U/U_t < 2.754$, $2.8 < (G_s/\rho_g U) < 14$, $0.176 < (H_d/H_b) < 0.727$. The heat transfer ratio was in the range of 0.241 to 0.752.

6. Conclusions

In the present experimental program on a single vertical tube located at various axial positions in a CFB riser, the measured total surface-average convective heat transfer coefficients were in the range of 58 to 101 $W{\cdot}m^{-2}{\cdot}K^{-1}$ for a suspension density range of 10 to 42 $kg{\cdot}m^{-3}$. The heat transfer coefficient increased with increasing average suspension density and solid circulation flux but decreased with increasing gas velocity. The heat transfer coefficient varied with the location of the heat transfer tube even when the average suspension densities were equal, indicating that the local dynamics of gas and particles adjacent to the surface dictates the heat transfer coefficient. The gas convective component for core surfaces was found to be in the range of 30 to 80% of the total convective coefficients. The heat transfer ratio defined as the ratio of the gas convective component to the total convective coefficient increased with gas velocity, this being more prominent at higher locations. Empirical correlations were developed for the average heat transfer coefficient and the heat transfer ratio at the axial tube in terms of important design and operating parameters including a non-dimensional height parameter.

References

[1] S.L. Darling, A. Asinine, G. Shibagaki, Experience with in-furnace surface in CFB boilers, in: Proceedings of 13th International Conference on Fluidized Bed Combustion, Orlando, Florida, Vol. 1, 1995, pp. 9–16.

[2] L.R. Glicksman, Heat transfer in circulating fluidized beds, in: J.R. Grace, A.A. Avidan, T.M. Knowlton (Eds.), Circulating Fluidized Beds, Blackie Academic and Professional, London, 1996, pp. 261–311.

[3] A.K. Kolar, Heat transfer in circulating fluidized bed boilers: Perspective and issues, in: Proceedings of Fourth ISHMT–ASME Heat and Mass Transfer Conference, Tata McGraw-Hill, India, 2000, pp. 105–116.

[4] J.F. Davidson, R. Cliff, Fluidization, Academic Press, New York, 1985.

[5] K.D. Kiang, K.T. Liu, H. Nack, J.H. Oxley, Heat transfer in fast fluidized beds, in: Fluidization Technology, Vol. 2, Hemisphere, Washington, DC, 1975, pp. 471–483.

[6] P. Basu, Heat transfer in high temperature fast fluidized beds, Chemical Engrg. Sci. (1990) 3123–3136.

[7] Q.Y. Zheng, X. Wang, X. Li, Heat transfer in circulating fluidized bed, in: P. Basu, M. Horio, M. Hasatani (Eds.), Circulating Fluidized Bed Technology III, Pergamon Press, Canada, 1991, pp. 263–268.

[8] H. Bi, Y. Jin, Z. Yu, D. Bai, An investigation of heat transfer in CFB, in: P. Basu, M. Horio, M. Hasatani (Eds.), Circulating Fluidized Bed Technology III, Pergamon Press, Canada, 1991, pp. 233–238.

[9] G.R. Ahn, G.Y. Han, Bed-to-immersed tube heat transfer in a circulating fluidized bed, J. Chem. Engrg. Japan 30 (1997) 421–426.

[10] G. Mincic, B. Stojanovic, M. Stojiljkovic, B. Blagojevic, The influence of heat transfer surface location on heat transfer in circulating fluidized bed, in: 1st South-East European Symposium on Fluidized Beds in Energy Production, Chemical and Process Engineering and Ecology, Ohrid, Republic of Macedonia, 1997, pp. 335–344.

[11] R.C. Zijerveld, F. Johnsson, A. Marzocchella, J.C. Schouten, C.M. van den Bleek, Fluidization regimes and transitions from fixed bed to dilute transport flow, Powder Technology 95 (1998) 185–204.